since 1961

Baltica

BALTICA Volume 39 Number 1 June 2026: 16–24
https://doi.org/10.5200/baltica.2026.1.2

Research article

Base friction model test investigation of deformation modes of gently dipped layered surrounding rock

Yudong Li, Min Xia*, Jiayuan Fan, Qi Huang, Wenhui Zeng, Rongquan Fan

Li, Y., Xia, M., Fan, J., Huang, Q., Zeng, W., Fan, R. 2026. Base friction model test investigation of deformation modes of gently dipped layered surrounding rock. *Baltica 39 (1)* 16–24. Vilnius. ISSN 0067-3064.

Manuscript submitted 18 June 2025 / Accepted 21 January 2026 / Available online 23 February 2026

Abstract. This study investigates the deformation and failure mechanisms of gently layered surrounding rock during underground excavation in a hydropower station in Shaanxi Province, China, through base friction physical simulation tests. Results indicate rock mass instability is governed by weak discontinuities (layer planes, joints, and faults). Four failure modes emerge: (1) tensile crack collapse at the tunnel arch induced by stress concentration, (2) shear slip at the sidewalls and shoulders due to exceeding shear strength, (3) bulging deformation of thin-layered rock under compressive stress, and (4) slight uplift at the invert of the main powerhouse due to upward pressure. The physical simulation tests replicate the deformation and failure evolution of the surrounding rock mass during excavation. Initially, the process is characterized by tunnel arch spall and slight slip, progressing to rock mass collapse due to structural plane coalescence. The study reveals the complex mechanical behaviour of failure in gently layered surrounding rock. The tunnel arch exhibits a "tension crack collapse – shear slip – bedding" failure mode, while the sidewall is primarily influenced by shear slip. Findings confirm discontinuities' control on the stability of layered surrounding rock, offering guidance for deformation support and long-term maintenance. These results provide significant theoretical and practical implications for engineering applications.

Keywords: *tunnel; gently-inclined layered rock mass; physical simulation; failure mechanisms*

Yudong Li, Min Xia (xiamin15@cdut.edu.cn), https://orcid.org 0000-0003-3621-3422
State Key Laboratory of Geohazard Prevention and Geoenvironment Protection (Chengdu University of Technology), Chengdu, Sichuan
State Grid Sichuan Electric Power Company, Chengdu, Sichuan
Southwest University of Science and Technology, Mianyang, Sichuan

**Corresponding author*

INTRODUCTION

The deformation and failure of surrounding rock in underground tunnels are controlled by lithological properties and discontinuities within the rock mass. For layered surrounding rock, the spatial arrangement of discontinuities governs stability, inducing failure modes including bulging, tensile crack collapse, and shear slip that threaten engineering safety. The underground powerhouses in hydropower projects have relatively high requirements for controlling the deformation of the rock mass (Bewick 2021). Therefore, it is imperative to investigate the mechanisms underlying deformation and failure during excavation in layered rock masses. Current research investigates excavation-induced deformation and failure of surrounding rock through numerical simulation, physical simulation, and in-situ monitoring.

Duan *et al*. (2017) investigated the failure mechanism of rock masses influenced by weak interlayers in large underground caverns, using extensive field monitoring data. Zhao *et al*. (2024) demonstrated the impact of weak interlayers on the stability of surrounding rock through a combination of in-situ monitoring, laboratory testing, and numerical simulations. Physical and numerical simulations have become predominant due to in-situ monitoring's time-consuming and high costs.

Lu *et al*. (2023) revealed the failure mechanism of layered surrounding rock through numerical modelling, establishing failure modes based on principal stress-bedding relationships. Wang *et al*. (2024) investigated the spalling failure mechanism of tunnels, using numerical simulation. Chen (2024) described fault impacts on rock stability through numerical analysis. Hao (2013) demonstrated interlayer shear stress-strength disparity as the key control of delamination, using composite beam theory-based simulations. Sha *et al*. (2023) investigated failure mechanisms of a horizontal layered tunnel arch through equivalent plate-beam modelling. Ma *et al*. (2024) revealed the deformation and failure mechanism of tunnel surrounding rock through physical modelling. Liu *et al*. (2015) identified phased deformation evolution characteristics through coupled physical-numerical methodologies. Sun *et al*. (2024) analyzed the deformation-failure mechanism of jointed tunnel surrounding rock, using integrated physical and numerical simulations. These studies provide fundamental theoretical frameworks for layered surrounding rock deformation and failure mechanisms.

This study simulates the deformation and failure progression of an underground tunnel in a hydropower project (Shaanxi Province, China). Through systematic investigation of the geological context and deformation-failure patterns of underground excavation, the research reveals the deformation mechanism governing layered surrounding rock failure.

GEOLOGICAL CHARACTERISTICS OF SURROUNDING ROCK IN UNDERGROUND POWERHOUSES

The prototype hydropower station is situated on the northern bank of the Weihe River in Shaanxi Province, China, with a site elevation ranging from 740 m to 1200 m, exhibiting a moderate-high mountain terrain. The underground powerhouse comprises the main powerhouse (180 m × 28.5 m × 56 m, axis SW 212°), the main transformer chamber (153.5 m × 19.5 m × 22.3 m, axis SW 212°), and a tailrace surge chamber (128 m × 10 m × 37.6 m, axis SW 212°).

The main powerhouse and the main transformer chamber employ gallery-type configurations, while the tailrace surge chamber features a cylindrical design. Borehole logging indicates the tunnel arch of the main powerhouse and the main transformer chamber intersect horizontal layered thin limestone (thickness: 0.07–0.15 m), while the remaining sections exhibit horizontal layered medium-thick limestone (thickness: 0.3–0.6 m).

The engineering area is mainly developed with bedding plane J1 (NE 50–75°/NW ∠ 0–5°, crack aperture 0.2–0.3 cm), joint J2 (NW 305°/NE ∠ 84°, aperture 0.1–0.2 cm), and joint J3 (NE 40–80°/SE ∠ 86°, aperture 0.2–0.3 cm). The steeply dipping J2 and J3 structural planes constitute a conjugate joint system. Field investigations revealed three faults in the underground powerhouse area: F1 (NE 60°/SE ∠

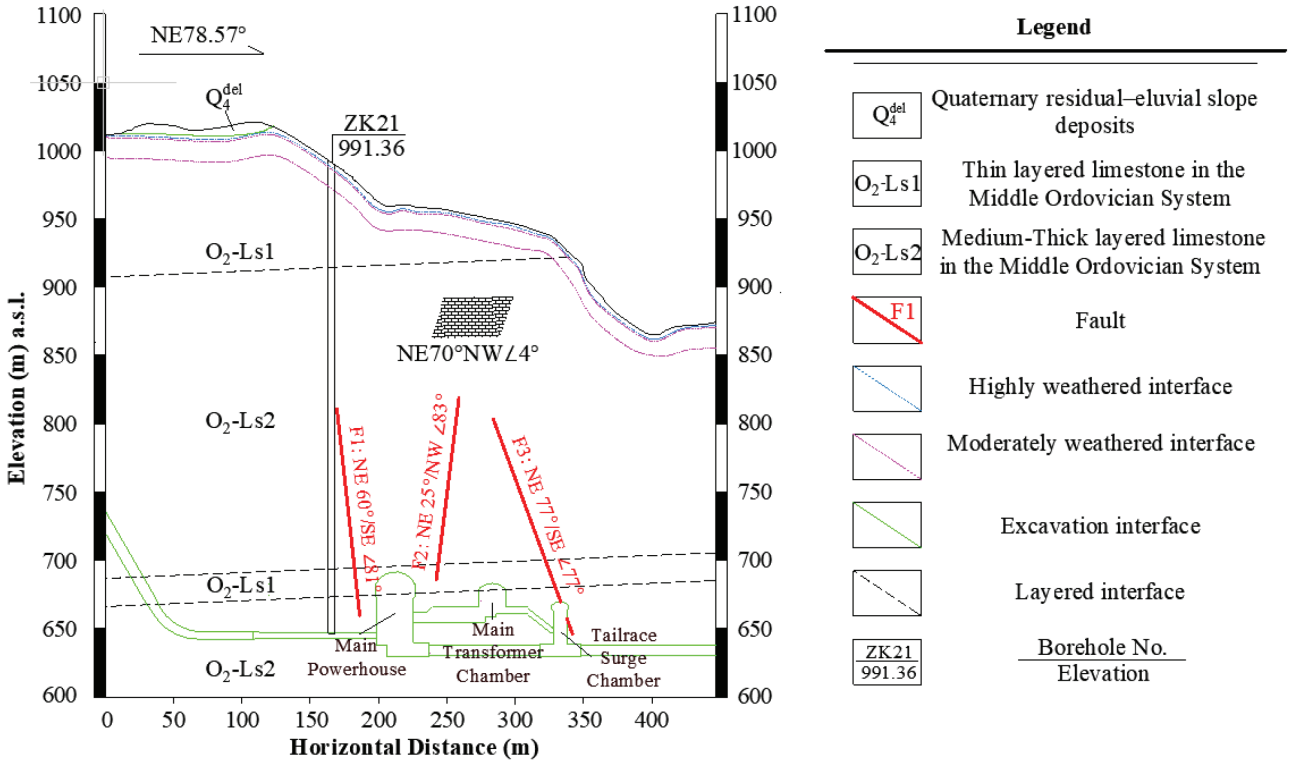

Fig. 1 Engineering geological cross-section

81°), F2 (NE 25°/NW ∠ 83°), and F3 (NE 77°/SE ∠ 77°). Notably, the F3 fault intersects and penetrates the tailgate surge chamber. The engineering geological cross-section is presented in Fig. 1.

DEFORMATION AND FAILURE MODES OF SURROUNDING ROCK

Influencing factors of stability of surrounding rock

Physical and mechanical properties of rock

The physical and mechanical properties of rock masses play a critical role in the stability of surrounding rock. These properties influence rock mass instability through various mechanisms, with strength parameters such as tensile strength and shear strength directly determining the load-bearing capacity of the rock masses. In situations where well-developed structural planes are present, rocks with lower strength are prone to deformation and failure (Wang *et al*. 2024).

Structural configuration and geological discontinuities in rock masses

The structural configuration and geological discontinuities of rock govern their deformation and failure, combined with their physical and mechanical properties. Faults and joints within rock masses induce structural fragmentation. Additionally, layered rock masses exhibit distinct mechanical properties due to variations in layer thickness. Consequently, the deformation and failure tendencies of layered rock masses are more pronounced compared to those of homogeneous rock formations (Xue 2023; Tu 2018).

Geomechanical analysis of deformation and failure modes

Tensile-crack collapse

Upon excavation of an underground tunnel, the free surface is created. Due to self-weight and unloading effects, the tensile stress in the rock mass at the free surface gradually exceeds the tensile strength of the rock mass. Consequently, the rock mass undergoes cracking and eventual collapse, with the failure predominantly manifesting as new tensile crack surfaces. An example of this failure mechanism is spalling observed at the shoulder of the tunnel (Fig. 2a).

Shear slip

Shear slip failure occurs when shear stress along a structural plane exceeds its shear strength. This failure mode is frequently observed in underground powerhouses due to the presence of faults and joints. Primary failure initiates with tunnel excavation, forming a free surface on the sidewall. Two joint sets intersect gentle layer J1 (crack 1: NE 55°/NW 70°, crack 2: NW 346°/SW 85°) (Fig. 2b).

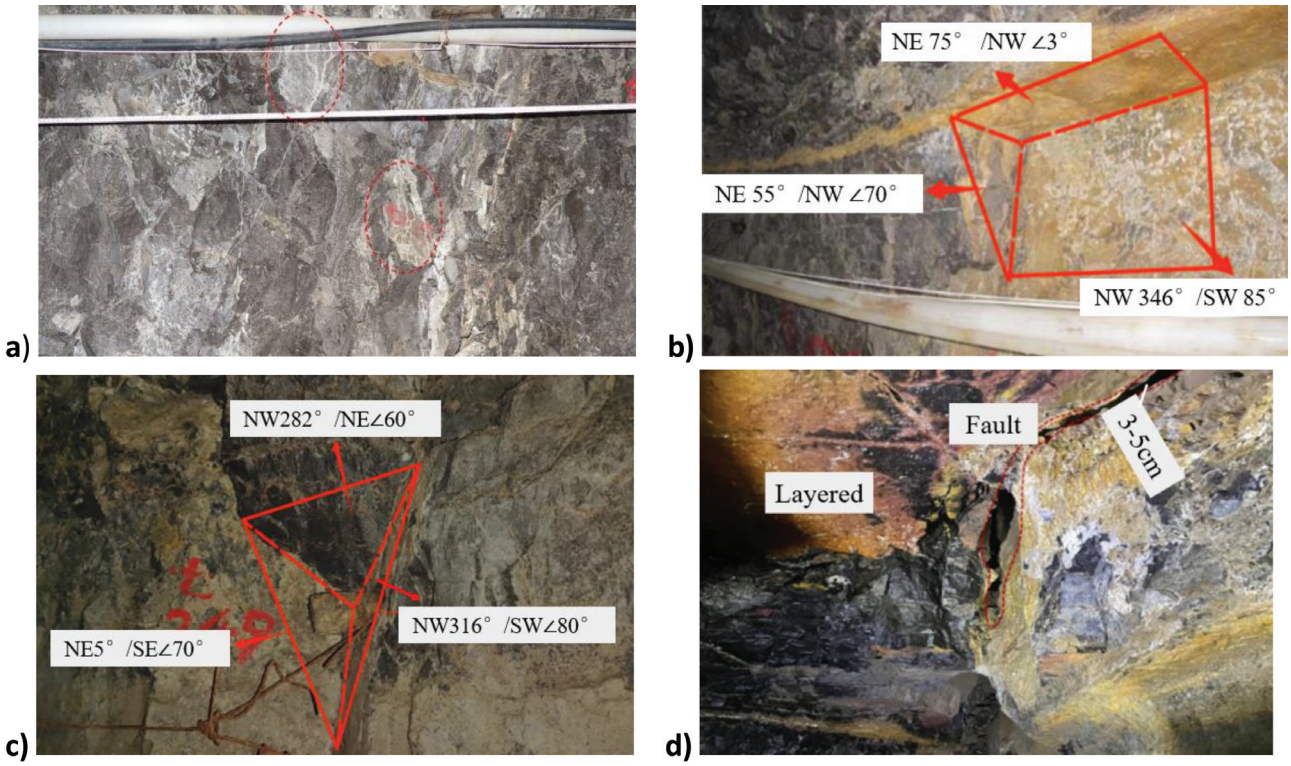

Fig. 2 Typical deformation modes based on investigation in exploration adit: a) tensile-crack collapse, b) shear slip, c) wedge failure, d) bulging

Wedge failure

Wedge failure is formed by the excavation of a tunnel and the intersection of three sets of secondary joints: crack 3 (NW282°/NE 60°), crack 4 (NW316°/SW 80°), and crack 5 (NE5°/SE 70°) (Fig. 2c). Due to the presence of the free surface, the excavated rock mass collapses under gravity.

Bulging

At the crown of an underground tunnel, thinly layered rock masses experience deformation due to excavation-induced compressive stress concentration (Fig. 2d). A steeply dipping fault develops at the crown (SW202°/SE 85°), which further fractures the thinly layered horizontal rock masses, generating cracks with apertures of 3 to 5 cm.

BASE FRICTION MODEL TESTS

Method and test device

Based on the principle of similarity, physical simulation tests should ensure that the physical test results of the model are similar to the prototype. The base friction test, as a prevalent gravity simulation technique, operates by replacing gravity with friction within the model. The schematic diagram and experimental device are showed in Fig. 3.

According to Saint-Venant's principle, when the model is sufficiently thin, the friction force resulting from its movement can be assumed to act uniformly across the entire thickness of the model, which effectively replicates the gravity loading conditions under natural circumstances.

The fully automated base friction test machine developed by Chengdu University of Technology was employed to test (Cai et al. 2008). By adhering to similarity principles, the scaled model simulates the prototype geological mass, ensuring observed physical phenomena align with natural laws.

Materials preparation and proportions

The selection of similitude materials for the base friction test was guided by similarity criteria. In this study, limestone was selected as the prototype for the surrounding rock masses. The simulation material is made by an intimate mixture of barite powder (fine aggregate), quartz powder (coarse aggregate) and liquid paraffin (binder) (Xu *et al*. 2021). The ratio of the compositions is 60.1% : 30.7% : 9.2% for barite powder, quartz powder, and paraffin oil (Fig. 4, Table 1). The similitude coefficients of unit weight (γ) and internal friction angle (φ) between the scaled model and prototype geological mass approached 1.

Table 1 Ratio of the compositions for base friction model test

Ratio of the compositions (%)		
Barium sulfate	Quartz sand	Liquid Paraffin
60.1	30.7	9.2

Table 2 Physical and mechanical properties of the prototype and physical models

Properties	Unit weight γ	Cohesion c	Internal friction angle φ
Limestone prototype	27.4 kN/m^3	0.75 MPa	45°
Physical models	27.45 kN/m^3	21.34 kPa	45°

This study investigates deformation-failure mechanisms in layered surrounding rock through physical modelling. The scaled model (C_L = 200) incorporates a gently dipped layer (J1), two steep joint sets (J2 and J3), and three faults (F1–F3). Experimental parameters adhere to stress similarity ratio (C_σ) of 200 and strain similarity ratio (C_ε) of 1, based on field investigation data.

Due to a small spacing between joints, a conventional base friction model for layered rock cannot be created by cutting the joints with a knife. Therefore, the spacing of joint sets is determined by considering the actual connectivity ratio. Specifically, the spacing

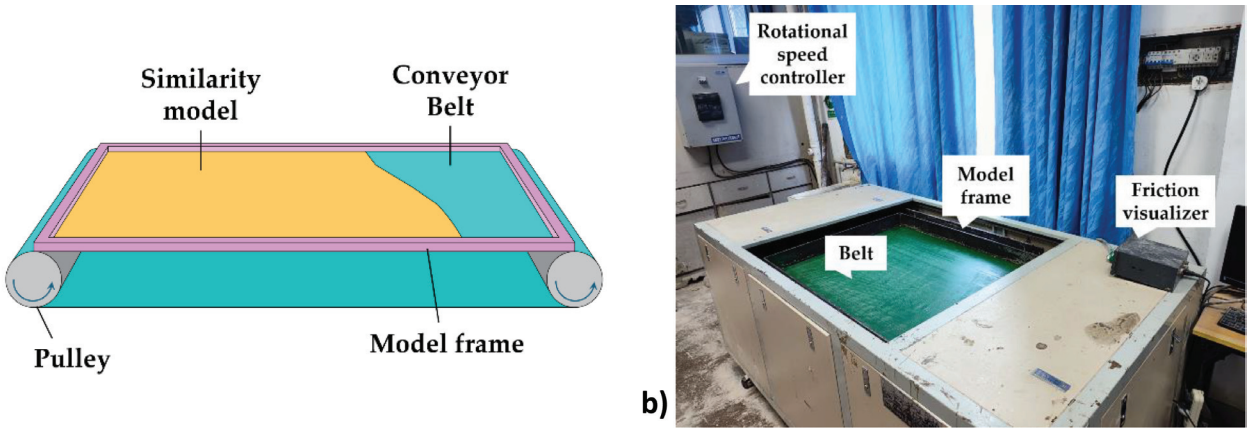

Fig. 3 Schematic diagram and equipment of base friction model test: a) schematic diagram, b) test equipment

Fig. 4 Base friction model test material formulation

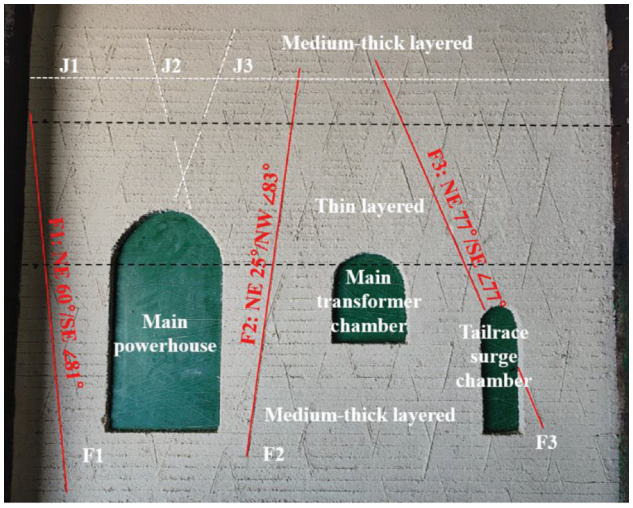

Fig. 5 Physical model used for base-friction test

for the horizontal layer J1 is set to 1 cm and 1.5 cm for thin and medium-thick layers, respectively, with a connectivity ratio of 100%. The spacing for the steep, hard joint sets J2 and J3 is 5 cm each, with connectivity ratios of 60–70%. Figure 5 illustrates a simplified model of the rock mass with a layered structure exhibiting base friction.

RESULTS AND ANALYSIS

The physical simulation test conducted in this study elucidates the deformation process of horizontal layered surrounding rock. The findings indicate that the deformation and failure of caverns, induced by excavation and self-weight, primarily concentrate on the tunnel arch and sidewalls. Additionally, a slight uplift is observed in the floor of the main powerhouse. These deformation and failure are predominantly governed by the horizontal layer (J1) and two sets of steeply dipped discontinuities (J2 and J3).

The main powerhouse experiences shear slip, slight uplift and bulging failure, while the main transformer chamber undergoes shear slip, tensile crack collapse, and bulging failure. The tailrace surge chamber only exhibits shear slip when subjected to the combined effects of the top arch horizontal layer and fault F3, resulting in the smallest scale of deformation failure (Fig. 6). Simulated evolution and results are delineated as follows:

Bulging

According to the simulation results, the bulging failure of surrounding rock occurs at the top arch of the main powerhouse and the main transformer chamber, as the rotation of the belt induces the formation of micro cracks in the thin layered surrounding rock at the top of the main powerhouse and the main transformer chamber (Fig. 7). Simultaneously, a sagging moment is produced. As the cracks widen, the sagging moment progressively intensifies. Consequently, the top arch horizontal spall occurred, leading to crack widths ranging from 5 mm to 7 mm.

Tensile-crack collapse

At the top arch of the main powerhouse and the main transformer chamber, there is a noticeable increase in tangential stress, while radial stress gradually diminishes and eventually approaching zero. During the ongoing base friction test, the tensile stress on the tunnel arch surpasses the tensile strength of the rock, resulting in the formation of tensile cracks in the horizontal layer, causing instability in rock mass until collapse ensues (Fig. 8).

Shear slip

Shear slip failure in the main powerhouse at the left sidewall of the tunnel is governed by J1 and J2. As the belt rotates, the crack resulting from the layer spall of J1 progressively widens until intersects J2, shear slip occurs in the rock, ultimately collapsing towards the tunnel's base, thereby creating a new free surface conditions for subsequent shear slip events. The shear slip deformation of the sidewall of the main transformer chamber is due to the widening crack of J1, until it intersects J3 (Fig. 9).

Slight uplift

Based on simulation results, slight uplift deformation occurs at the invert of the main powerhouse. As showed in Fig. 10, belt rotation generates upward pressure at the tunnel invert, while the combination of discontinuities J2 and J3 induces slight uplift deformation along these discontinuities.

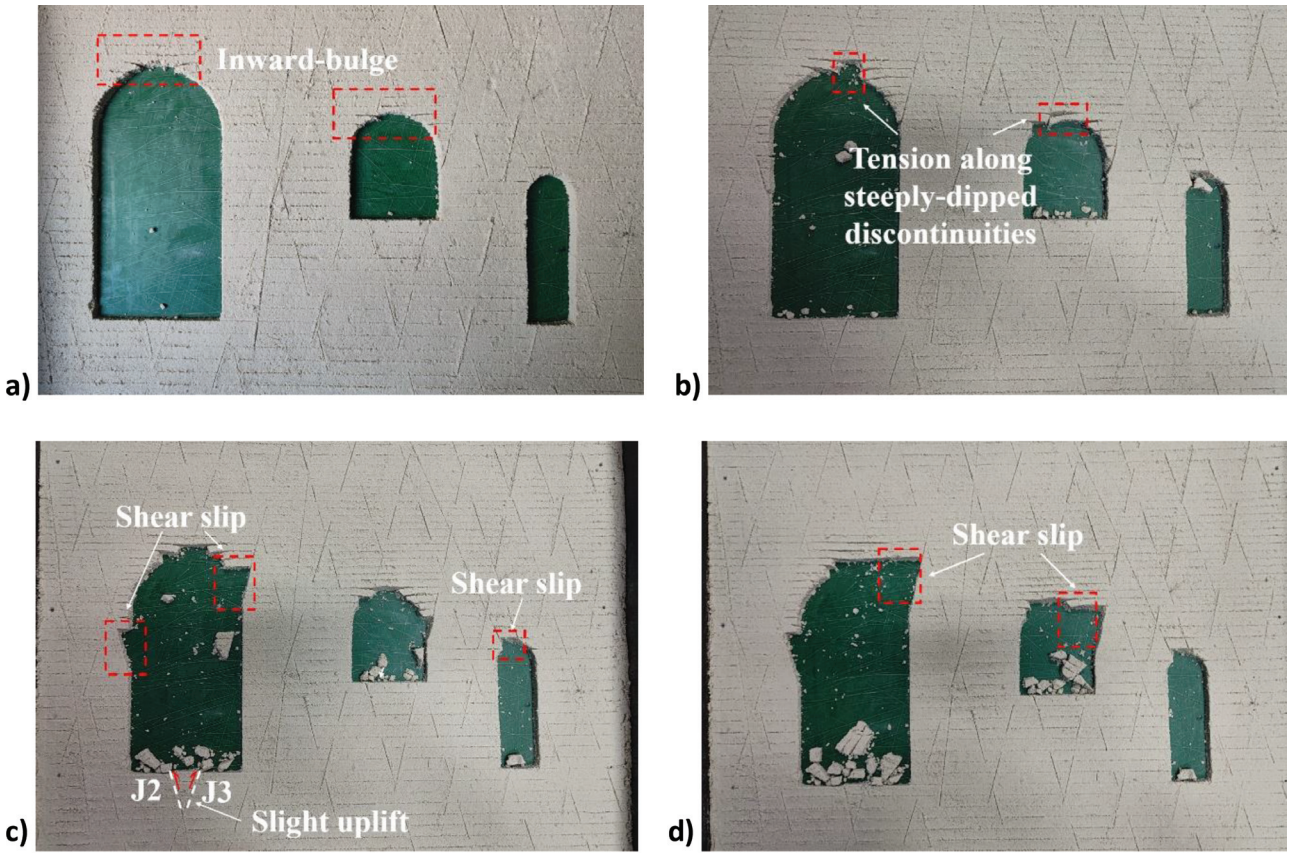

Fig. 6 Deformation evolution process of surrounding rock revealed by base-friction model tests: a) roof strata bulging inward, b) tension along steeply dipping discontinuities, c) shear slip and localized slight uplift, d) deformation characteristics after experiment completion

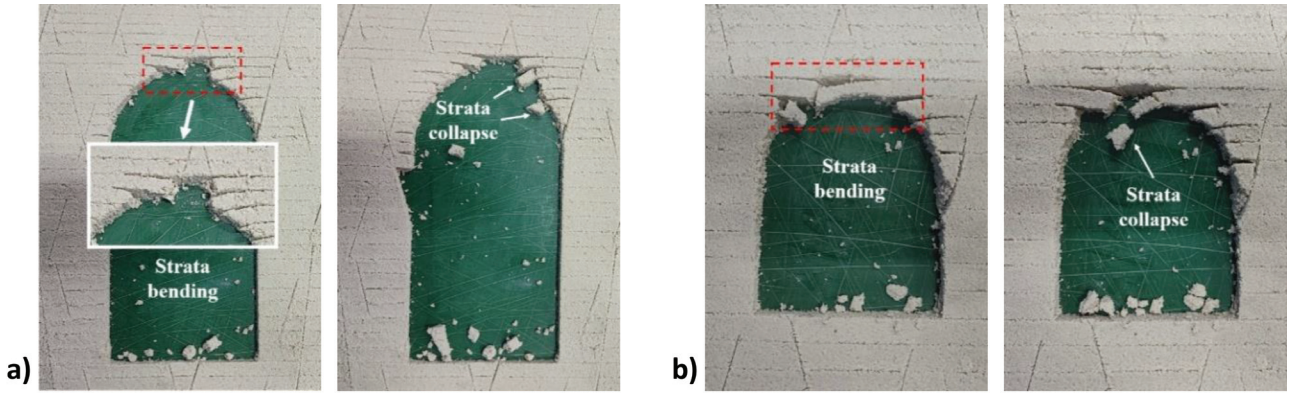

Fig. 7 Deformation characteristics of bulging: a) main powerhouse, b) main transformer chamber

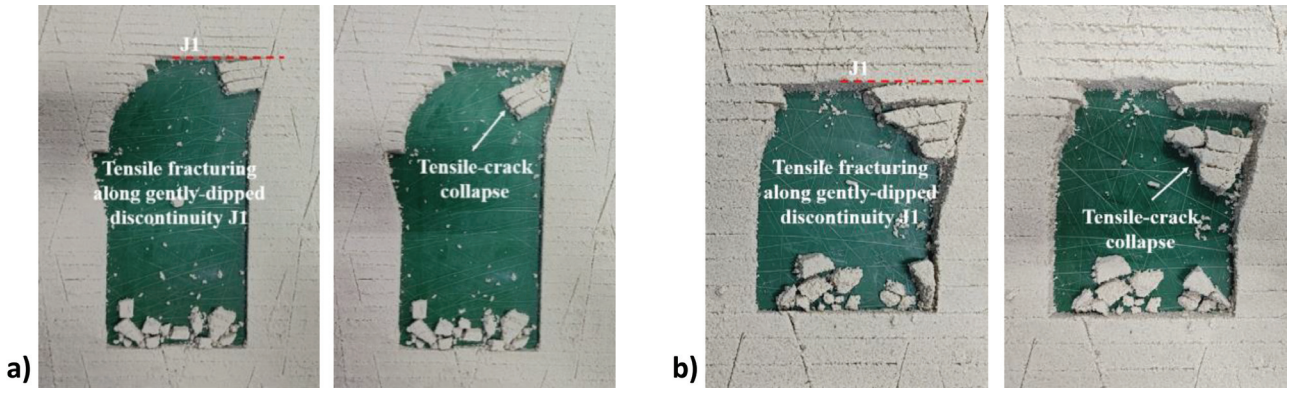

Fig. 8 Deformation characteristics of tensile-crack collapse: a) main powerhouse, b) main transformer chamber

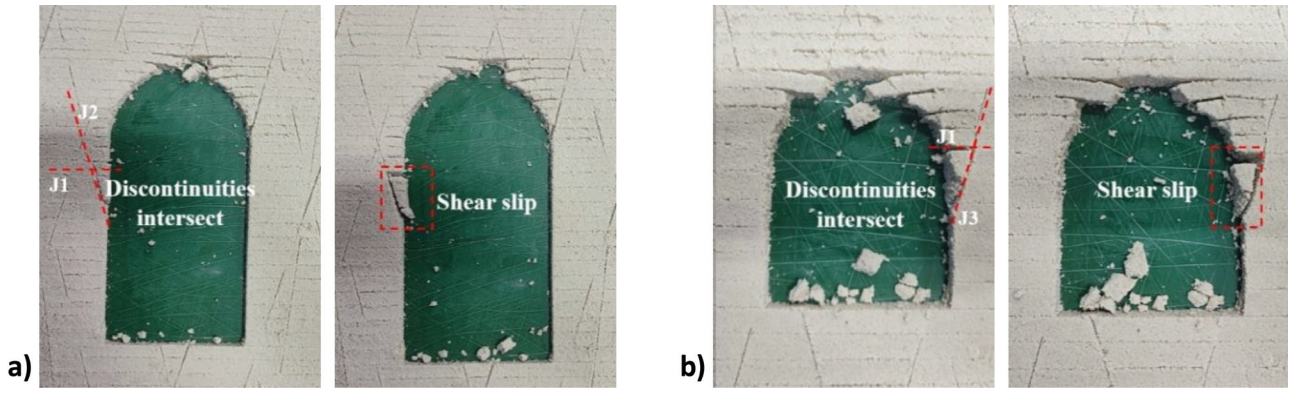

Fig. 9 Deformation characteristics of shear slip: a) main powerhouse, b) main transformer chamber

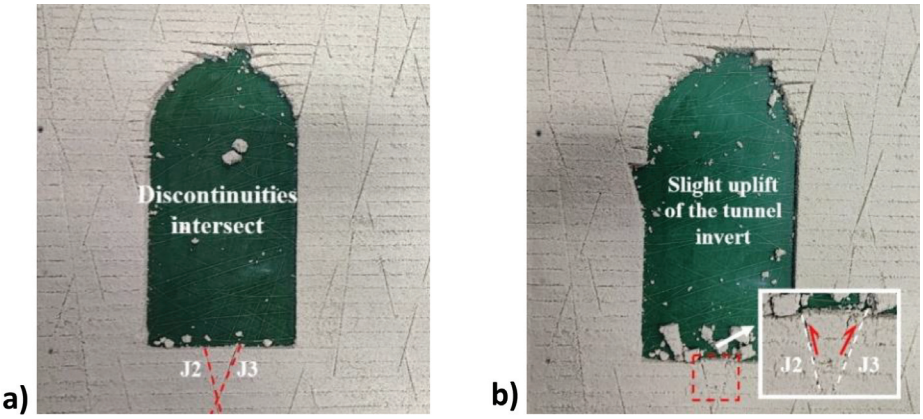

Fig. 10 Deformation characteristics of slight uplift occurring in the cave floor

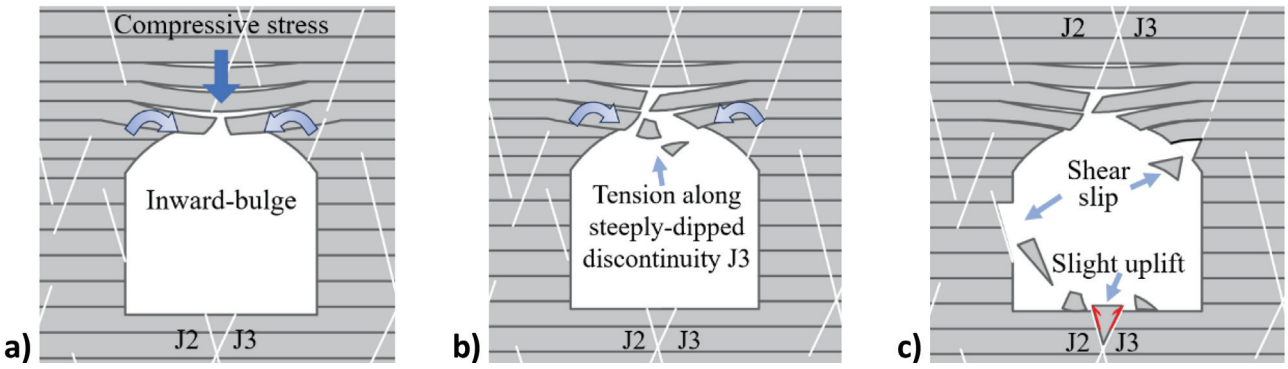

Fig. 11 Deformation and failure mechanism diagrams a) bulging, b) tensile-crack collapse, c) shear slip and slight uplift

DISCUSSING: GEOMECHANICAL MODEL OF GENTLY DIPPED LAYERED SURROUNDING ROCK

The surrounding rock of underground tunnel attains a stable triaxial stress state following geological processes and deformation over an extended period (Li *et al*. 2025). Human engineering activities, such as cavern excavation, induce stress alterations in these regions, leading to gradual deformation and failure of the surrounding rock. The subsequent analysis delves into the mechanisms of deformation and failure.

Following the excavation of the cavern, the horizontal layers of rock surrounding the top arch will inward bulge due to unloading and self-weight (Fig. 11a). As tensile stress in the rock intensifies, fracture spacing widens and extends. Once the tensile stress surpasses the tensile strength of the rock mass, it loses integrity and undergoes tensile fracture collapse failure, detaching from the parent rock (Fig. 11b).

When the roof arch collapses, the stress is transferred to the sidewall and shoulder of the cavern. The surrounding rock of the sidewall and shoulder is influenced by the layer and two joints, leading to the formation of rock blocks. Shear stress causes gradual shear slip deformation along the shear plane between the sidewall and the shoulder. Shear slip failure occurs when the shear stress surpasses the shear strength, causing the rock block to slide and result in collapse (Fig. 11c).

As the free surface extends, a cantilever beam effect emerges due to weakened support conditions, causing a concentration of shear stress along joints, leading to secondary tensile collapse failure.

Simultaneously, slight uplift occurs in the invert of the main powerhouse due to the influence of two discontinuities (J1 and J2) and tangential pressure (Fig. 11c). Throughout the deformation process, deformation primarily occurs at joint-wall intersections (Zhang 2021; Zhang, Zhang 2021).

Ultimately, a composite failure mode of tension crack collapse – shear slip – bulging in the tunnel arch, while shear slip failure predominantly occurring in the sidewall.

CONCLUSION

The deformation and failure mechanism of the gently layered rock surrounding the underground powerhouse of a hydropower station in Shaanxi Province were investigated through the base friction test. The main conclusion was obtained as follows:

(1) The geological analysis of deformation and failure modes in the layered surrounding rock reveals four types: bulging failure, tensile crack collapse failure, wedge failure, and shear slip failure.

(2) The deformation and failure of the layered surrounding rock, as observed in physical simulations under self-weight, are influenced by various cracks. These planes manifest as collapse, shear slip failure, and bulging in the top arch rock, as well as slip failure in the sidewall and slight uplift failure at the invert of the main powerhouse. The failure mechanism can be described as follows: the tunnel arch exhibits a composite failure mode involving tensile crack collapse, shear slip, and bulging, while the sidewall demonstrates a shear slip failure mode.

ACKNOWLEDGMENTS

This study was supported by the National Natural Science Foundation of China (U23A20651). The authors sincerely thank the Editor and the reviewers for their comments which greatly improved the quality of the manuscript.

Conflict of interests

The authors have no competing interests to declare that are relevant to the content of this article.

REFERENCES

Bewick, R.P. 2021. The Strength of Massive to Moderately Jointed Rock and its Application to Cave Mining. *Rock Mechanics and Rock Engineering 54*, 3629–3661. https://doi.org/10.1007/s00603-021-02466-3

Cai, G., Huang, R., Yan, M., Gong, M. 2008. Physical simulation study on deformation and failure response of an anti-inclined slope during excavation. *Chinese Journal of Rock Mechanics and Engineering 04*, 811–817. https://doi.org/10.3321/j.issn:1000-6915.2008.04.022

Chen, Y. 2024. Study on Ground Stress Characteristics and Tunnel Deformation Control Technology in Fault Area, M. Sc. thesis, Shijiazhuang-Tiedao University, Shijiazhuang, China. https://doi.org/10.27334/d.cnki.gstdy.2024.000460

Duan, S., Feng, X., Jiang, Q., Liu, G., Pei, S., Fan, Y. 2017. In Situ Observation of Failure Mechanisms Controlled by Rock Masses with Weak Interlayer Zones in Large Underground Cavern Excavations Under High Geostress. *Rock Mechanics and Rock Engineering 50*, 2465–2493. https://doi.org/10.1007/s00603-017-1249-4

Hao, G. 2013. Deformation Mechanism and Finite Analysis of Tunnel in Horizontal Layered Rockmass. *Railway Construction Technology 06*, 30–34 + 49. https://doi.org/10.3969/j.issn.1009-4539.2013.06.010

Li, S., Zhang, S., Li, Y., Liu, X., Li, Z., Xu, D., Cheng, L., Jiang, Q., Tang, D., Chen, G. 2025. Failure mechanism and stability control of hard rock in extremely high stress large underground powerhouse of Shuangjiangkou hydropower station. *Rock and Soil Mechanics 46(5)*, 1–14. https://doi.org/10.16285/j.rsm.2024.1234

Liu, P., Ji, F., Wen, S. 2015. Simulation Study on the Deformation and Failure Mechanism of Level Rock in Tunnels. *Modern Tunnelling Technology 52(3)*, 82–87. https://doi.org/10.13807/j.cnki.mtt.2015.03.012

Lu, S., Sun, Z., Zhang, D., Liu, C., Wang, J., Huangfu, N. 2023. Numerical modelling and field observations on the failure mechanisms of deep tunnels in layered surrounding rock. *Engineering Failure Analysis 153*, 1–27. https://doi.org/10.1016/j.engfailanal.2023.107598

Ma, X., Zhai, Z., Xiang, J., Wei, M., Tian, Z., Chen, L. 2024. Research on Deformation and Failure Mechanism of Surrounding Rock in Inclined Strata with Soft-Hard Interbedded Roadways. *Rock Mechanics and Rock Engineering 57*, 11319–11332. https://doi.org/10.1007/s00603-024-04128-6

Sha, J., Ye, Y., Yao, N. 2023. Study on Deformation and Failure Characteristics and Mechanism of Surrounding Rock in Roadways with Different Inclination Stratiform Rock Masses. *Metal. Mine 12*, 62–68. https://doi.org/10.19614/j.cnki.jsks.202312010

Sun, B., Mei, Y., Li, W., Zhang, C., Shao, X., Li, T., Li, W., Zhao, W., Wang, L. 2024. Experimental study on the deformation and failure mode of surrounding rocks of a tunnel in a jointed rock mass. *Engineering. Failure Analysis 163(A)*, 1–18. https://doi.org/10.1016/j.engfailanal.2024.108470

Tu, H. 2018. Research on the Stability and Failure Mechanism of Horizontal Layered Surrounding Rock Tunnel. *Journal of Railway Engineering Society 9*, 75–79 + 87. https://doi.org/10.3969/j.issn.1006-2106.2018.09.013

Wang, X., Lv, X., Liang, M., Meng, J. 2024. Research

on the Deformation Law and Progressive Failure Mechanism of Horizontal Layered Surroundings Rock. *Science & Technology Information 8*, 140–142. https://doi.org/10.16661/j.cnki.1672-3791.2401-5042-6942

Wang, Y., Zhang, Q., Yuan, L., Wang, X., Wang, S., Wei, L. 2024. Spalling Failure Mechanism of Surrounding Rock in Deep Hard-Rock Tunnels. *Geotechnical and Geological Engineering 42*, 7225–7242. https://doi.org/10.1007/s10706-024-02924-z

Xu, Z., Luo, Y., Chen, J., Su, Z., Zhu, T., Yuan, J. 2021. Mechanical properties and reasonable proportioning of similar materials in physical model test of tunnel lining cracking. *Construction and Building Materials* (*300*), 1–13. https://doi.org/10.1016/j.conbuildmat.2021.123960

Xue, X. 2023. Deformation and Failure Mechanism of TBM Excavated Roadway in Deep Jointed Strata of Coal Mine and Control Countermeasures. PhD dissertation, China University of Mining and Technology, Xuzhou, China. https://doi.org/10.27623/d.cnki.gzkyu.2023.000033

Zhang, B. 2021. Analysis of Unloading Deformation and Failure and Supporting Effect of Non-persistent Jointed Surrounding Rock. M. Sc. thesis, Taiyuan University of Technology, Taiyuan, China. https://doi.org/10.27352/d.cnki.gylgu.2021.000952

Zhang, B., Zhang, C. 2021. Numerical Analysis on the Influence of Non-persistent Joint Inclination on the Deformation and Failure of Surrounding Rock. *Journal of Taiyuan University of Technology 52(5)*, 789–796. https://doi.org/10.16355/j.cnki.issn1007-9432tyut.2021.05.013

Zhao, J., Chen, B., Jiang, Q., Xu, D., He, B., Duan, S. 2024. In-situ comprehensive investigation of deformation mechanism of the rock mass with weak interlayer zone in the Baihetan hydropower station. *Tunneling Underground Space Technol 148*, 1–16. https://doi.org/10.1016/j.tust.2024.105690